A Mixed Integer Linear Programming-based Distributed Energy Management for Three-phase Unbalanced Active Distribution Network

Guodong Liu, Maximiliano Ferrari
Electrification and Energy Infrastructures Division
Oak Ridge National Laboratory
Oak Ridge, TN 37831 USA
Email: liug@ornl.gov, ferrarimagmf@ornl.gov

Yang Chen
Dept. of Industrial and Systems Engineering
North Carolina Agricultural and Technical State University
Greensboro, NC 27411 USA
Email: ychen1@ncat.edu

***Abstract*—A mixed integer linear programming (MILP)–based distributed energy management for three-phase unbalanced active distribution network is proposed. Modern distribution networks have becoming more and more active with increasing deployment of microgrids, distributed energy resources (DERs) as well as controllable loads. Considering various ownership and control models of microgrids, DERs and controllable loads, a distributed energy management was formulated using the alternating direction method of multipliers (ADMM) algorithm. By ADMM, the distribution management system (DMS) and these active components are coordinated through price signals, which are adjusted according to the generation-load mismatch per node per phase. To enable resolution of the ADMM-based distributed optimization using more accessible and popular MILP solver, different linearization techniques were proposed to linearize the augmented Lagrangian terms and other nonlinear terms. Results of case studies on a three-phase active distribution network with three microgrids and several DERs and controllable loads validated the effectiveness of proposed MILP-based distributed energy management. In addition, the capability of proposed method in mitigating phase power unbalance has been demonstrated.**

***Index Terms*—Distributed optimization, energy management, networked microgrids, three-phase distribution network**

NOMENCLATURE

The bold symbols stand for corresponding vectors/matrices. (k) on the upper right position indicates *k*-th iteration. ϕ on the lower right position indicates the phase ϕ value.

A. Indices

m	Index of microgrids, from 1 to N_M.
g	Index of distributed generators (DGs) in microgrid m/distribution network, from 1 to N_G^m/N_G^{DN}.
l	Index of controllable loads in microgrid m/distribution network, from 1 to N_L^m/N_L^{DN}.
b	Index of batteries in microgrid m/distribution network, from 1 to N_B^m/N_B^{DN}.
w	Index of wind turbines in microgrid m, from 1 to N_W^m.
v	Index of PV in microgrid m, from 1 to N_V^m.
n	Index of buses/nodes in the distribution network, from 1 to N_N.
f	Index of distribution feeders, from 1 to N_F.
i	Index of energy blocks of DGs, from 1 to N_I.
t	Index of time intervals, from 1 to N_T.
ϕ	Index of phases, from 1 to N_Φ.

B. Variables

u_{mgt}	Binary indicator of unit g's on/off status.
$u_{mbt}^{\mathrm{C}}, u_{mbt}^{\mathrm{D}}$	Binary indicator of battery b's charging/discharging status.
$p_{mgt}(i)$	Scheduled power in i-th energy block offer by DG g in microgrid m during period t.
P_{mgt}, Q_{mgt}	Scheduled real/reactive power of DG g in microgrid m.
$P_{m\phi t}^{\mathrm{PCC}}, Q_{m\phi t}^{\mathrm{PCC}}$	Scheduled real/reactive power at point of common coupling (PCC) of microgrid m on phase ϕ.
$P_{mbt}^{\mathrm{C}}, P_{mbt}^{\mathrm{D}}$	Scheduled charging/discharging power of battery b in microgrid m during period t.
Q_{mbt}	Scheduled reactive power of battery b in microgrid m during period t.
SOC_{mbt}	State of charge (SOC) of battery b.
$P_{mvt}^{\mathrm{PV}}, P_{mwt}^{\mathrm{W}}$	Power output of PV panel v /wind turbine w in microgrid m during period t.
$P_{ml\phi t}^{\mathrm{LS}}, Q_{ml\phi t}^{\mathrm{LS}}$	Scheduled real/reactive load shedding of load l in microgrid m on phase ϕ during period t.
$V_{n\phi t}$	Voltage magnitude of bus n on phase ϕ during period t.
$P_{f\phi t}^{\mathrm{F}}, Q_{f\phi t}^{\mathrm{F}}$	Real/reactive power flow in feeder f phase ϕ during period t.
$P_{\phi t}^{\mathrm{SB}}, Q_{\phi t}^{\mathrm{SB}}$	Real/reactive injection at the distribution substation on phase ϕ during period t.
$V_{\phi t}^{\mathrm{SB}}$	Voltage magnitude of the distribution substation on phase ϕ during period t.

C. Constants

$\lambda_{mgt}(i)$	Marginal cost of the i-th energy block offer by DG g during period t.
$\lambda_t^{\mathrm{SB,P}}, \lambda_t^{\mathrm{SB,Q}}$	Price of real/reactive power at distribution substation during period t.
C_{mbt}	Degradation cost of battery b in microgrid m during period t.
$C_{ml\phi t}$	Curtailment cost of load l on phase ϕ during period t.

This manuscript has been authored by UT-Battelle, LLC under Contract No. DE-AC05-00OR22725 with the U.S. Department of Energy. The United States Government retains and the publisher, by accepting the article for publication, acknowledges that the United States Government retains a non-exclusive, paid-up, irrevocable, world-wide license to publish or reproduce the published form of this manuscript, or allow others to do so, for United States Government purposes. The Department of Energy will provide public access to these results of federally sponsored research in accordance with the DOE Public Access Plan (http://energy.gov/downloads/doe-public-access-plan).

$p_{mg}^{\max}(i)$ Maximum power of the i-th energy block by DG g in microgrid m.
$P_{mg}^{\min}, P_{mg}^{\max}$ Minimum/maximum power of DG i in microgrid m.
$P_{m\phi}^{\mathrm{PCC,max}}$ Maximum power of microgrid m on phase ϕ at PCC.
$P_{\phi}^{\mathrm{SB,max}}$ Maximum exchanged power at the distribution substation on phase ϕ during period t.
$P_{mb}^{\mathrm{C,max}}, P_{mb}^{\mathrm{D,max}}$ Maximum charging/discharging power of battery b in microgrid m.
$SOC_{mbt}^{\min}, SOC_{mbt}^{\max}$ SOC limits of battery b in microgrid m.
$\eta_{mb}^{\mathrm{C}}, \eta_{mb}^{D}$ Charging/discharging efficiency of battery b.
$P_{ml\phi t}, Q_{ml\phi t}$ Estimated real/reactive power of load l in microgrid m on phase ϕ during period t.
$\alpha_{ml\phi t}$ Maximum shedding percentage of load l in microgrid m on phase ϕ during period t.
κ_{mg} Operating Cost of DG g in microgrid m at the running power of $P_{mg}^{\min}$.
$V_{\mathrm{thr}}^{\min}, V_{\mathrm{thr}}^{\max}$ Voltage thresholds beyond which voltage deviation will be penalized.
$V^{\min}, V^{\max}$ Minimum/maximum voltage limits.
V^{Fix} Fixed voltage magnitude at the distribution substation bus.
r_{jk}^{aa}, x_{jk}^{aa} Self resistance and reactance of Phase a of line from bus j to bus k.
r_{jk}^{ab}, x_{jk}^{ab} Mutual resistance and reactance between Phase a and Phase b of line from bus j to bus k.
$S_{mg}, S_{mb}, S_{f\phi}$ Capacity limit of DG g, battery b and feeder f on phase ϕ.
$\tan(\theta_{mg})$ Power factor limit of DG g in microgrid m.
$\tan(\varphi_{ml\phi})$ Power factor of load l in microgrid m.
γ_t Maximum phase unbalance power in period t.
$A^{\mathrm{SB}}, A^{\mathrm{PCC}}, A^{\mathrm{F}}$ Incidence matrix for substation bus injections, microgrids and distribution feeders.
$A^{\mathrm{DN,G}}, A^{\mathrm{DN,B}}, A^{\mathrm{DN,L}}$ Incidence matrix for DGs, batteries and loads that directly connected to the distribution network.

I. Introduction

With the steadying decline in costs of distributed energy resources (DERs) driven by improved manufacturing efficiencies and reduction of hardware costs, locally installed distributed generators (DGs), e.g., rooftop PV systems, and energy storage systems (ESSs), e.g., customer owned batteries have become vastly more affordable across the U.S. As of the end of 2022, the total capacity of PV installed in the U.S. has grown from 2.1 GW (in 2010) to 110.1 GW [1]. As a result. the traditional passive distribution networks become active ones with increasing penetration of DERs and microgrids.

Although the increasing penetration of DERs enables a low-carbon future, secure and efficient operation of active distribution network requires careful coordination of distribution network and associated active components, i.e., DERs, microgrids and controllable loads. Generally, existing research could be divided into two groups: centralized and distributed [2]. Centralized approaches normally utilize a multi-level hierarchical framework, which coordinates multiple microgrids, load/DER aggregators through an optimal power flow in the upper level and schedules the DERs and loads in each microgrid or load/DER aggregator in the lower level [3]. A bi-level energy management system was proposed to cooperate the operation of multiple solid-state power substations in active distribution networks [4]. More popularly, the energy management of active distribution network is realized in distributed methods, which preserve the privacy and autonomy of microgrids and DER/load aggregators [5]. A distributed energy management for balanced distribution network with various actively interfaced participants, including DERs, flexible loads, and different kinds of microgrids using the alternating direction method of multipliers (ADMM) algorithm was proposed in [6]. Considering the three-phase distribution network, a transactive energy-based distributed energy management is proposed to coordinate the operation of networked microgrids in [7].

Existing work on distributed energy management of active distribution networks are mainly utilizing a quadratic augmented Lagrangian term introduced by ADMM to drive the convergence of the distributed optimization, which requires commercial mixed integer conic programming (MICP) solvers, such as CPLEX [8] or GUROBI [9] to solve the subproblems. In [10], a piecewise linearization technique was proposed to transform the quadratic augmented Lagrangian term into mixed integer linear (MIL) form so that the proposed optimization could be solved by free and open-source MILP solvers, e.g., COIN-OR Branch and Cut solver (CBC) [11]. However, the distribution network has been neglected in [10]. To enable the resolution of ADMM-based distributed optimization using more accessible and popular MILP solver while still considering the three-phase unbalanced distribution network, a MILP-based distributed energy management for three-phase unbalanced active distribution network is proposed by linearizing the augmented Lagrangian terms and other nonlinear terms using various linearization techniques. The main contribution of this work includes:

1) A MILP-based distributed energy management for three-phase unbalanced active distribution network with embedded DERs and microgrids is proposed.
2) The proposed MILP-based distributed energy management are validated on a three-phase active distribution network with several microgrids and DERs. The capability of proposed method in mitigating phase power unbalance has been demonstrated.

Section II and III describes the centralized energy management and proposed MILP-based distributed energy management for three-phase unbalanced active distribution network. In Section IV, results of case studies are presented and analyzed. Finally, Section V concludes the paper.

II. Centralized Energy Management

A centralized energy management of active distribution network is formulated in this section. The objectives include minimizing total operating costs as well as optimizing other performance indices, e.g., voltage deviations and reactive power exchanged at the distribution substation, as in (1). In specific, the system total operating costs includes the operating cost of DGs, ESS and controllable loads in all microgrids (line 1-4), operating cost of DGs, ESS and controllable loads directly interfaced with the distribution network (line 4-7), and the energy exchanging cost/benefit at distribution substation (line 8). The system performance indices include total voltage deviations (line 9-10) and total absolute value of reactive power exchange at distribution substation (line 11), which

reflects the power factor at distribution substation. Note that W_C, W_V and W_Q are weighting coefficients.

$$\begin{aligned}\min \quad & W_C \left\{ \sum_{t=1}^{N_T} \sum_{m=1}^{N_M} \sum_{g=1}^{N_G^m} \left[\sum_{i=1}^{N_I} \lambda_{mgt}(i) p_{mgt}(i) + \kappa_{mg} u_{mgt} \right] \right. \\ & + \sum_{t=1}^{N_T} \sum_{m=1}^{N_M} \sum_{g=1}^{N_G^m} SU_{mgt}\left(u_{mgt}, u_{mg,t-1}\right) \\ & + \sum_{t=1}^{N_T} \sum_{m=1}^{N_M} \sum_{b=1}^{N_B^m} C_{mbt} \left(P_{mbt}^{\mathrm{C}} + P_{mbt}^{\mathrm{D}} \right) \\ & + \sum_{t=1}^{N_T} \sum_{m=1}^{N_M} \sum_{l=1}^{N_L^m} \sum_{\phi=1}^{N_\Phi} C_{ml\phi t} P_{ml\phi t}^{LS} \\ & + \sum_{t=1}^{N_T} \sum_{g=1}^{N_G^{\mathrm{DN}}} \left[\sum_{i=1}^{N_I} \lambda_{gt}(i) p_{gt}(i) + \kappa_g u_{gt} \right] \\ & + \sum_{t=1}^{N_T} \sum_{g=1}^{N_G^{\mathrm{DN}}} SU_{gt}\left(u_{gt}, u_{g,t-1}\right) \\ & + \sum_{t=1}^{N_T} \sum_{b=1}^{N_B^{DN}} C_{bt} \left(P_{bt}^{\mathrm{C}} + P_{bt}^{\mathrm{D}} \right) + \sum_{t=1}^{N_T} \sum_{l=1}^{N_L^{DN}} \sum_{\phi=1}^{N_\Phi} C_{l\phi t} P_{l\phi t}^{LS} \\ & \left. + \sum_{t=1}^{N_T} \sum_{\phi=1}^{N_\Phi} \lambda_t^{\mathrm{SB,P}} P_{\phi t}^{\mathrm{SB}} \right\} \\ & + W_V \left[\sum_{t=1}^{N_T} \sum_{n=1}^{N_N} \sum_{\phi=1}^{N_\Phi} V_{n\phi t}^2 - (V_{\mathrm{thr}}^{\max})^2 : (V_{n\phi t} > V_{\mathrm{thr}}^{\max}) \right. \\ & \left. + \sum_{t=1}^{N_T} \sum_{n=1}^{N_N} \sum_{\phi=1}^{N_\Phi} \left(V_{\mathrm{thr}}^{\min} \right)^2 - V_{n\phi t}^2 : (V_{n\phi t} < V_{\mathrm{thr}}^{\min}) \right] \\ & + W_Q \left(\sum_{t=1}^{N_T} \sum_{\phi=1}^{N_\Phi} \lambda_t^{\mathrm{SB,Q}} \left| Q_{\phi t}^{\mathrm{SB}} \right| \right) \end{aligned} \tag{1}$$

s.t.

$$P_{mgt} = \sum_{i=1}^{N_I} p_{mgt}(i) + u_{mgt} P_{mg}^{\min} \quad \forall m, \forall g, \forall t \tag{2}$$

$$0 \le p_{mgt}(i) \le p_{mg}^{\max}(i) \quad \forall m, \forall g, \forall t, \forall i \tag{3}$$

$$u_{mgt} P_{mg}^{\min} \le P_{mgt} \le u_{mgt} P_{mg}^{\max} \quad \forall m, \forall g, \forall t \tag{4}$$

$$-\tan(\theta_{mg}) P_{mgt} \le Q_{mgt} \le \tan(\theta_{mg}) P_{mgt} \quad \forall m, \forall g \tag{5}$$

$$(P_{mgt})^2 + (Q_{mgt})^2 \le S_{mg}^2 \quad \forall m, \forall g, \forall t \tag{6}$$

$$P_{mg\phi t} = P_{mgt}/N_\Phi \quad \forall m, \forall g, \forall t \tag{7}$$

$$Q_{mg\phi t} = Q_{mgt}/N_\Phi \quad \forall m, \forall g, \forall t \tag{8}$$

$$0 \le P_{mbt}^{\mathrm{C}} \le P_{mb}^{\mathrm{C,max}} u_{mbt}^{\mathrm{C}} \quad \forall m, \forall b, \forall t \tag{9}$$

$$0 \le P_{mbt}^{\mathrm{D}} \le P_{mb}^{\mathrm{D,max}} u_{mbt}^{\mathrm{D}} \quad \forall m, \forall b, \forall t \tag{10}$$

$$u_{mbt}^{\mathrm{C}} + u_{mbt}^{\mathrm{D}} \le 1 \quad \forall m, \forall b, \forall t \tag{11}$$

$$SOC_{mbt} = SOC_{mb,t-1} + P_{mbt}^{\mathrm{C}} \eta_{mb}^{\mathrm{C}} \triangle t - P_{mbt}^{\mathrm{D}} / \eta_{mb}^{\mathrm{D}} \triangle t \tag{12}$$

$$SOC_{mbt}^{\min} \le SOC_{mbt} \le SOC_{mbt}^{\max} \quad \forall m, \forall b, \forall t \tag{13}$$

$$\left(P_{mbt}^{\mathrm{D}} - P_{mbt}^{\mathrm{C}} \right)^2 + (Q_{mbt})^2 \le S_{mb}^2 \quad \forall m, \forall b, \forall t \tag{14}$$

$$P_{mb\phi t}^{\mathrm{C}} = P_{mbt}^{\mathrm{C}}/N_\Phi \quad \forall m, \forall b, \forall t \tag{15}$$

$$P_{mb\phi t}^{\mathrm{D}} = P_{mbt}^{\mathrm{D}}/N_\Phi \quad \forall m, \forall b, \forall t \tag{16}$$

$$Q_{mb\phi t} = Q_{mbt}/N_\Phi \quad \forall m, \forall b, \forall t \tag{17}$$

$$0 \le P_{ml\phi t}^{LS} \le \alpha_{ml\phi t}\% P_{ml\phi t} \quad \forall m, \forall l, \forall \phi, \forall t \tag{18}$$

$$Q_{ml\phi t}^{LS} = tan\left(\varphi_{ml\phi}\right) P_{ml\phi t} \quad \forall m, \forall l, \forall \phi, \forall t \tag{19}$$

$$P_{m\phi t}^{\mathrm{PCC}} = \sum_{g=1}^{N_G^m} P_{mg\phi t} + \sum_{b=1}^{N_B^m} \left(P_{mb\phi t}^{\mathrm{D}} - P_{mb\phi t}^{\mathrm{C}} \right) + \sum_{v=1}^{N_V^m} P_{mvt}^{\mathrm{PV}}/N_\Phi + \sum_{w=1}^{N_W^m} P_{mwt}^{\mathrm{W}}/N_\Phi - \sum_{l=1}^{N_L^m} \left(P_{ml\phi t} - P_{ml\phi t}^{LS} \right) \quad \forall m, \forall \phi \tag{20}$$

$$Q_{m\phi t}^{\mathrm{PCC}} = \sum_{g=1}^{N_G^m} Q_{mg\phi t} + \sum_{b=1}^{N_B^m} Q_{mb\phi t} - \sum_{l=1}^{N_L^m} \left(Q_{ml\phi t} - Q_{ml\phi t}^{LS} \right) \tag{21}$$

$$-P_{m\phi}^{\mathrm{PCC,max}} \le P_{m\phi t}^{\mathrm{PCC}} \le P_{m\phi}^{\mathrm{PCC,max}} \quad \forall m, \forall \phi, \forall t \tag{22}$$

$$\left(P_{m\phi t}^{\mathrm{PCC}} \right)^2 + \left(Q_{m\phi t}^{\mathrm{PCC}} \right)^2 \le \left(S_{m\phi}^{\mathrm{PCC}} \right)^2 \quad \forall m, \forall \phi, \forall t \tag{23}$$

$$\mathbf{V}_{jt}^2 = \mathbf{V}_{kt}^2 - \mathbf{M}_{jk}^{\mathrm{P}} \mathbf{P}_{jkt} + \mathbf{M}_{jk}^{\mathrm{Q}} \mathbf{Q}_{jkt} \quad \forall t \tag{24}$$

$$\mathbf{M}_{jk}^{\mathrm{P}} = \begin{bmatrix} -2r_{jk}^{aa} & r_{jk}^{ab} - \sqrt{3}x_{jk}^{ab} & r_{jk}^{ac} + \sqrt{3}x_{jk}^{ac} \\ r_{jk}^{ab} + \sqrt{3}x_{jk}^{ab} & -2r_{jk}^{bb} & r_{jk}^{bc} - \sqrt{3}x_{jk}^{bc} \\ r_{jk}^{ac} - \sqrt{3}x_{jk}^{ac} & r_{jk}^{bc} + \sqrt{3}x_{jk}^{bc} & -2r_{jk}^{cc} \end{bmatrix} \tag{25}$$

$$\mathbf{M}_{jk}^{\mathrm{Q}} = \begin{bmatrix} -2x_{jk}^{aa} & x_{jk}^{ab} + \sqrt{3}r_{jk}^{ab} & x_{jk}^{ac} - \sqrt{3}r_{jk}^{ac} \\ x_{jk}^{ab} - \sqrt{3}r_{jk}^{ab} & -2x_{jk}^{bb} & x_{jk}^{bc} + \sqrt{3}r_{jk}^{bc} \\ x_{jk}^{ac} + \sqrt{3}r_{jk}^{ac} & x_{jk}^{bc} - \sqrt{3}r_{jk}^{bc} & -2x_{jk}^{cc} \end{bmatrix} \tag{26}$$

$$\begin{aligned} A^{\mathrm{F}} \mathbf{P}^{\mathbf{F}} = \; & A^{\mathrm{SB}} \mathbf{P}^{\mathbf{SB}} + A^{\mathrm{DN,G}} \mathbf{P}^{\mathbf{G}} + A^{\mathrm{DN,B}} \mathbf{P}^{\mathbf{B}} \\ & - A^{\mathrm{PCC}} \mathbf{P}^{\mathbf{PCC}} - A^{\mathrm{DN,L}} \mathbf{P}^{\mathbf{L}} \quad \forall t \end{aligned} \tag{27}$$

$$\begin{aligned} A^{\mathrm{F}} \mathbf{Q}^{\mathbf{F}} = \; & A^{\mathrm{SB}} \mathbf{Q}^{\mathbf{SB}} + A^{\mathrm{DN,G}} \mathbf{Q}^{\mathbf{G}} + A^{\mathrm{DN,B}} \mathbf{Q}^{\mathbf{B}} \\ & - A^{\mathrm{PCC}} \mathbf{Q}^{\mathbf{PCC}} - A^{\mathrm{DN,L}} \mathbf{Q}^{\mathbf{L}} \quad \forall t \end{aligned} \tag{28}$$

$$\left(V^{\min} \right)^2 \le V_{n\phi t}^2 \le (V^{\max})^2 \quad \forall n, \forall \phi, \forall t \tag{29}$$

$$\left(P_{f\phi t}^{\mathrm{F}} \right)^2 + \left(Q_{f\phi t}^{\mathrm{F}} \right)^2 \le \left(S_{f\phi}^{\mathrm{F}} \right)^2 \quad \forall f, \forall \phi, \forall t \tag{30}$$

$$V_{\phi t}^{\mathrm{SB}} = V^{\mathrm{Fix}} \quad \forall \phi, \forall t \tag{31}$$

$$-P_{\phi}^{\mathrm{SB,max}} \le P_{\phi t}^{\mathrm{SB}} \le P_{\phi}^{\mathrm{SB,max}} \quad \forall \phi, \forall t \tag{32}$$

$$\left(P_{\phi t}^{\mathrm{SB}} \right)^2 + \left(Q_{\phi t}^{\mathrm{SB}} \right)^2 \le \left(S_{\phi}^{\mathrm{SB}} \right)^2 \quad \forall \phi, \forall t \tag{33}$$

$$-\gamma_t \le P_{\phi t}^{\mathrm{SB}} - P_{\phi' t}^{\mathrm{SB}} \le \gamma_t \quad \forall \phi, \forall \phi' \ne \phi, \forall t \tag{34}$$

The objective function is subject to various constraints. The constraints of DGs are represented as (2)-(8). The phase characteristics of DG outputs are represented in (7) and (8). Depending on the DG outputs are three-phase balanced or single-phase, N_Φ is set as 3 or 1. The constraints of ESSs are represented as (9)-(14). Like DGs, the phase characteristics of an ESS are represented in (15), (16) and (17). As to controllable loads, the maximum percentage of load shedding is enforced by (18) and (19).

For microgrids, the DGs, ESSs and controllable loads inside a microgrid are also subject to constraints (2)-(19). In addition, both real and reactive power of a microgrid should be balanced for each phase as enforced by (20) and (21). The power and capacity limits at the PCC are limited by (22) and (23).

The three-phase distribution network power flow is modeled using linearized three-phase distribution power flow (*LinDist3Flow*) model, which was originally proposed in [12] and represented in (24) - (30). The distribution substation is taken as the slack bus with fixed voltage magnitude as in (31). The real power and capacity of each phase at the substation are limited by (32) and (33), separately. To reduce the zero-sequence current and avoid mal-operation of zero-sequence protection, power between phases should be well balanced, as shown in (34). In summary, the centralized energy management for networked microgrids could be reformulated as a mixed-integer conic programming (MICP) as in [7].

III. Distributed Counterpart and Linearization

The ADMM-based distributed counterpart of the centralized optimization was proposed in [7]. For simplicity, the centralized energy management is represented in the form of (35)-(36), where x includes the variables in the upper level, e.g., distribution substation power, load/DERs directly interfaced with the distribution network, and the distribution network power flow, and z includes the variables in the lower level, e.g., load/DERs in each microgrid/aggregators.

$$Min \quad f(x)+g(z) \tag{35}$$

$$s.t. \quad Ax+Bz=c \tag{36}$$

First, the augmented Lagrangian function is formulated as in (37) by integrating the equality constraint (36), which corresponds to (27) and (28) in the centralized model.

$$\begin{aligned} L_\rho(x,z,y) &= f(x)+g(z)+y^T(Ax+Bz-c) \\ &\quad +\frac{\rho}{2}\|Ax+Bz-c\|_2^2 \end{aligned} \tag{37}$$

Then, the ADMM consists of the following iterations:

$$x^{k+1} = argmin_x L_\rho\left(x,z^k,y^k\right) \tag{38}$$

$$z^{k+1} = argmin_z L_\rho\left(x^{k+1},z,y^k\right) \tag{39}$$

$$y^{k+1} = y^k+\rho\left(Ax^k+Bz-c\right) \tag{40}$$

The ADMM utilizes a quadratic augmented Lagrangian term as in (37) to drive the convergence. In addition, quadratic capacity constraints of components, i.e., (6), (14), (23), (30) and (33), are in the form of $P^2+Q^2 \le S^2$. To solve subproblem (38) and (39) , commercial MICP solver is needed.

To enable the resolution of ADMM-based distributed optimization using more accessible MILP solvers, a MILP-based distributed optimization is proposed by linearizing the augmented Lagrangian term and quadratic constraints, separately.

Taking the augmented Lagrangian term in (38) for example, this term is actually the square of the Euclidean norm of the updated primal residual vector. For simplicity, we define $\boldsymbol{\chi}=Ax+Bz^k-c$ with $\boldsymbol{\chi}=[\chi_1,\chi_2,\dots\chi_t,\dots\chi_{N_T}]$. Thus, we have $\|\boldsymbol{\chi}\|_2^2=\sum_{t=1}^{N_T}(\chi_t)^2$. Next, the quadratic function of χ_t is linearized using piecewise linearization as illustrated in Fig. 1a. First, the range of $|\chi_t|$ is divided into N_I end-to-end pieces as in (41). Inside each piece, the quadratic curve of $(\chi_t)^2$ is substituted by a linear segment with constant slope $s_t(i)$. Then, we get $(\chi_t)^2=\sum_{i=1}^{N_I}\chi_t(i)\,s_t(i)$ with $\bar{\chi}_t(1),\dots\bar{\chi}_t(N_I)$ and slope $s_t(i)$ as constants.

$$\begin{cases} |\chi_t|=\sum_{i=1}^{N_I}\chi_t(i) \\ 0\le\chi_t(1)\le\bar{\chi}_t(1) \\ 0\le\chi_t(2)\le\bar{\chi}_t(2)-\bar{\chi}_t(1) \\ \dots \\ 0\le\chi_t(N_I)\le\bar{\chi}_t(N_I)-\bar{\chi}_t(N_I-1) \\ \sum_{i=1}^{N_I}\chi_t(i)\ge\chi_t, \quad \sum_{i=1}^{N_I}\chi_t(i)\ge-\chi_t \end{cases} \tag{41}$$

As to the quadratic capacity constraints $P^2+Q^2\le S^2$, i.e., a circle in geometry, an inscribed equilateral polygon could be used to approximate it. An inscribed regular octagon is proposed to estimate the quadratic capacity constraints, as in Fig. 1b. Thus, the original quadratic capacity constraints will be substituted by the edges of the inscribed regular octagon.

After linearization, the subproblems in MICP format are recast into MILP format. Thus, the ADMM-base distributed energy management is transformed into MILP-based distributed energy management, which could be solved by easily-accessible open-source MILP solvers.

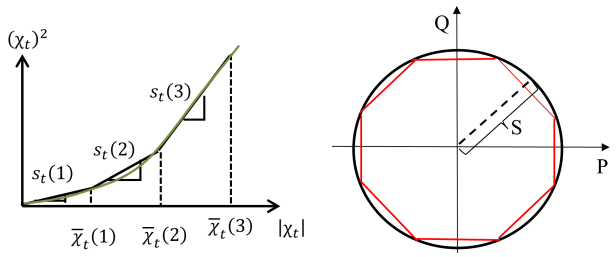

(a) Piecewise linearization of $(\chi_t)^2$ (b) Approximation of a circle

Fig. 1: Linearization techniques employed in the proposed MILP-based distributed optimization

IV. Case Studies

The proposed distributed energy management is demonstrated on a modified Oak Ridge National Laboratory (ORNL) test system, as shown in Fig. 2 [7]. Detailed parameters of the system and individual components could be found in [7]. The case studies is run for 24 hours, with hourly resolution. The voltage at distribution substation bus is assumed 1.0 p.u. and the initial price of all buses is set as 0.2 $/kWh. The penalty factor ρ is assumed 0.1. The optimization model is programmed in MATLAB and solved by the MICP solver CPLEX 12.6 and open-source MILP solver CBC, separately.

A. Comparing Objective Values and Solution Time

Using centralized method, ADMM-based distributed method and proposed MILP-based distributed method, various objective values and solution time are obtained and compared in Table I. Without loss of generality, the weighting coefficients are set as: $W_C=1$, $W_V=10$, and $W_Q=0.1$, for all cases. Comparing with centralized energy management, the total objective function calculated by the both distributed approaches are slightly increased by 4.31% and 4.15% in grid-connected mode, and 3.27% and 3.24% in islanded mode, separately. Meanwhile, the voltage

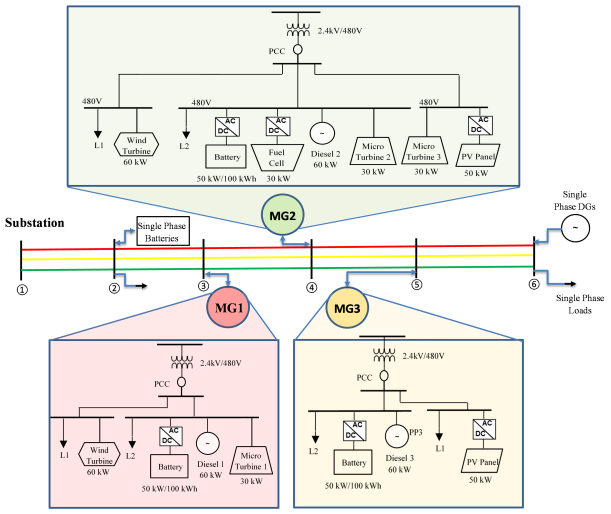

Fig. 2: Modified ORNL DECC microgrid system

TABLE I: Comparison of objectives and solution time of various methods for grid-connected(GC) and islanded(IS) modes

Cases		Total Obj. Value	Total Cost of DMS ($)	Total Cost of MGs ($)	Voltage Deviation (p.u.)	Var at Substation (k-Varh)	Solution Time (Seconds)
GC	Centr.	1020.90	432.47	568.62	0.20	178.04	31.42
	ADMM-based Distri.	1064.04	449.94	593.54	0.15	190.74	205.74
	MILP-based Distri.	1063.35	449.64	593.14	0.14	191.77	98.37
IS	Centr.	1624.25	377.93	1246.32	0	0	26.07
	ADMM-based Distri.	1677.30	446.55	1230.75	0	0	162.54
	MILP-based Distri.	1676.85	446.47	1230.38	0	0	76.28

deviation and reactive power exchanged at substation are almost the same. Comparing two distributed methods, the proposed MILP-based distributed method has reached nearly the same objective value as the ADMM-based distributed method. Therefore, the soundness of proposed MILP-based distributed method is validated. It should be noted that the solution time of proposed MILP-based method has been significantly reduced comparing with ADMM-based method. More importantly, the proposed MILP-based method could be solved by free and open-source MILP solvers, leading to accelerated deployment of DERs and microgrids.

B. Effects of Phase Balancing Constraints

First, the maximum phase unbalance power at the distribution substation γ_t was set as 20 kW (i.e., a large value). Using the MILP-based distributed method, the actual phase power injection at the distribution substation was obtained and shown in Fig. 3a. Then, γ_t was reduced to 10 kW. The phase power injection at substation was recalculated and shown in Fig. 3b. The actual maximum phase unbalance power of both cases are calculated and compared in Fig. 3c. As can be seen, the actual maximum phase unbalance power at the distribution substation bus have been reduced accordingly as γ_t was reduced to 10 kW. Thus, the capability of proposed method in mitigating phase power unbalance has been demonstrated.

For each phase, the average nodal price signals with different settings of γ_t are compared in Fig. 3d. Originally, Phase c is more heavily loaded than Phase a and b as shown in Fig. 3a. To reduce this phase power unbalance by setting $\gamma_t = 10$ kW, the single phase DGs on Phase c are committed to reduce the power injection of Phase c at the substation. As a result, the relatively expensive single phase DGs on Phase c elevate the average nodal price of Phase c. As to Phase a and b, the reduction of power injection of Phase c at the substation enables reduction of power injection of Phase a and b through increasing the discharging power of single-phase batteries at Phase a and b, which reduces the average nodal price of Phase a and b. In short, the nodal price of three phases are coupled.

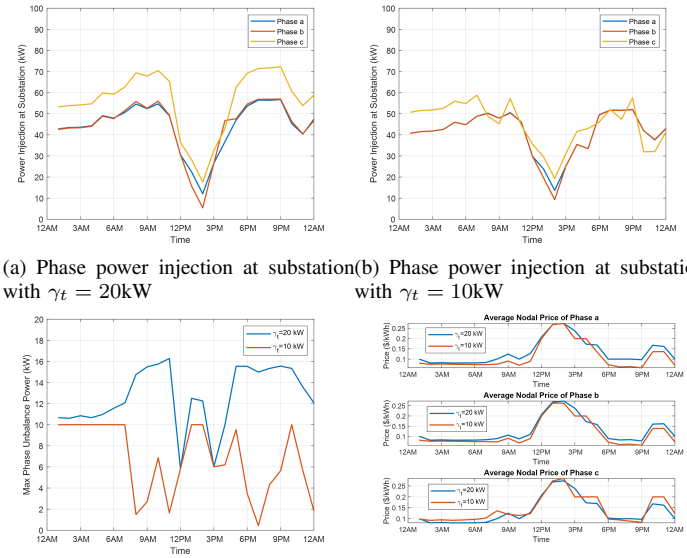

(a) Phase power injection at substation with $\gamma_t = 20$kW (b) Phase power injection at substation with $\gamma_t = 10$kW

(c) Maximum phase unbalance power (d) Average nodal price of three phases

Fig. 3: Comparison of phase power, maximum phase unbalance and average phase prices with different settings of γ_t

V. Conclusions

A MILP-based distributed energy management for three-phase active distribution network was proposed. Different linearization techniques were employed to transform the MICP into MILP. Results of case studies validated the proposed method.

References

[1] Solar Industry Research Data. Solar Energy Industries Association. [online] Available: https://www.seia.org/solar-industry-research-data.

[2] M. Islam, F. Yang, and M. Amin, "Control and optimisation of networked microgrids: A review." *IET Renew Power Gener.,* vol. 15, pp. 1133-1148, Feb. 2021.

[3] Z. Wang, B. Chen, J. Wang, M. M. Begovic and C. Chen, "Coordinated Energy Management of Networked Microgrids in Distribution Systems," *IEEE Trans. Smart Grid*, vol. 6, no. 1, pp. 45-53, Jan. 2015.

[4] G. Liu, R. Moorthy, J. Choi et al., "Linearised three-phase optimal power flow for coordinated optimisation of residential solid-state power substations", *IET Energy Syst. Integr.*, vol. 3, pp. 344-354, Jul. 2021.

[5] G. Liu, T. Jiang, T. Ollis, X. Zhang and K. Tomsovic, "Distributed energy management for community microgrids considering network operational constraints and building thermal dynamics," Appl. Energy, Vol. 239, pp. 83-95, Apr. 2019.

[6] G. Liu, T. Ollis, M. F. Ferrari, A. Sundararajan and Y. Chen, "Distributed Energy Management for Networked Microgrids Embedded Modern Distribution System Using ADMM Algorithm," *IEEE Access*, vol. 11, pp. 102589-102604, Sep. 2023.

[7] G. Liu, T. Ollis, M. Ferrari. et al. RETRACTED ARTICLE: "Distributed energy management for networked microgrids in a three-phase unbalanced distribution network," *Front. Energy* vol. 17, no. 446, Dec. 2022.

[8] The ILOG CPLEX Website. 2022. Available online: http://www- 01.ibm.com/software/commerce/optimization/cplexoptimizer/ index.html.

[9] Gurobi Optimizer. 2022. Available online: https://www.gurobi.com/products/gurobioptimizer/.

[10] G. Liu, M. Ferrari, T. B. Ollis, and K. Tomsovic, "An MILP-Based Distributed Energy Management for Coordination of Networked Microgrids," *Energies* vol. 15, no. 19, pp. 6971, Sep. 2022.

[11] CBC User Guide. 2022. Available online: https://www.coinor.org/Cbc/cbcuserguide.html (accessed on November 1, 2023).

[12] B. A. Robbins and A. D. Domínguez-García, "Optimal Reactive Power Dispatch for Voltage Regulation in Unbalanced Distribution Systems," *IEEE Trans. Power Syst.,* vol. 31, no. 4, pp. 2903-2913, Jul. 2016.